Optimization of the Separation of Sulfur Hexafluoride and Nitrogen by Selective Adsorption Using Monte Carlo Simulations

Santiago Builes
MATGAS Research Center (Carburos Metálicos/Air Products, CSIC, UAB), Campus de la UAB, 08193 Bellaterra, Spain

Institut de Ciència de Materials de Barcelona, Consejo Superior de Investigaciones Científicas, (ICMAB-CSIC), Campus de la UAB, 08193 Bellaterra, Spain

Thomas Roussel
Institut de Ciència de Materials de Barcelona, Consejo Superior de Investigaciones Científicas, (ICMAB-CSIC), Campus de la UAB, 08193 Bellaterra, Spain

Lourdes F. Vega
MATGAS Research Center (Carburos Metálicos/Air Products, CSIC, UAB), Campus de la UAB, 08193 Bellaterra, Spain

Institut de Ciència de Materials de Barcelona, Consejo Superior de Investigaciones Científicas, (ICMAB-CSIC), Campus de la UAB, 08193 Bellaterra, Spain

DOI 10.1002/aic.12312
Published online July 6, 2010 in Wiley Online Library (wileyonlinelibrary.com).

We present molecular simulations to find the optimal conditions for the separation by adsorption of SF_6 from a gaseous mixture with N_2, a mixture of key interest in electrical applications. The effect of pore size, pressure, and mixture compositions on the selective adsorption of SF_6 was investigated by using Grand Canonical Monte Carlo simulations with simple fluid models and a simplified model of MCM-41. Simulations performed with multisite fluid models confirm that general trends are predicted using simple models, including a maximum in SF_6 selectivity for pore diameters around 1.1 nm. Simulations were also performed using two atomistic models of zeolite-templated carbon (ZTC), FAU-ZTC, and EMT-ZTC, materials with average pore sizes close to 1.1 nm, obtaining high selectivities for both materials. Selectivities for FAU-ZTC are approximately four times higher than the best materials published for this mixture separation, opening excellent opportunities to use it for recovering SF_6 from SF_6/N_2 mixtures. *AIChE J,* 57: 962–974, 2011
Keywords: separation by adsorption, sulfur hexafluoride, nitrogen, molecular simulations, multisite force fields, MCM-41, zeolite-templated carbon materials

Introduction

Sulfur hexafluoride (SF_6) is a colorless, odorless, nontoxic, and nonflammable gas. It is mainly used in gas insulated substations and related equipment in electrical transmission

Correspondence concerning this article should be addressed to L. F. Vega at vegal@matgas.com.

and distribution systems because its arc quenching properties and high dielectric strength. Despite these unique properties, SF_6 is a very potent greenhouse gas (GHG); its global warming potential is 22,000 larger than carbon dioxide's and its atmospheric lifetime is estimated to be 3200 years.[1,2] Therefore, almost all SF_6 emissions need to be avoided because of its long-term effects in the environment. Hence, there have been numerous efforts to reduce emissions from facilities using SF_6.[3,4] Besides, there are numerous research studies aimed at finding an alternative gas for insulation of electrical equipment, but a suitable substitute for SF_6 for some key applications is yet to be found.[5–7]

One of the main options to diminish SF_6 emissions is mixing it with other gases to reduce the overall amount of SF_6 used, while keeping the desired properties of the pure fluid. Nitrogen is the preferred gas for these mixtures, for two main reasons: mixtures of SF_6 and N_2 with a low concentration of SF_6 still maintain the high dielectric strength of pure SF_6; and nitrogen is a cheap gas, making the overall process cheaper and environmentally friendlier.[8,9] However, a mixture of sulfur hexafluoride and nitrogen increases the difficulty of recovering and recycling the SF_6, as in this case a process able to effectively separate SF_6 and N_2 is required. The process becomes more complex as the amount of SF_6 in the mixture becomes very small.[8] Besides, the high concentration of N_2 in the gas mixtures used for insulation of electrical equipment makes the separation by liquefaction an unpractical process, since it requires an excessive amount of energy to cool down and pressurize the mixture; hence, alternative processes are required.

There are some works available in the literature dealing with the separation of the SF_6/N_2 mixtures, being most of them experimental studies using adsorbents. The separation of SF_6 from N_2 by adsorption is achieved either by molecularly sieving the N_2 or by preferentially adsorbing the SF_6 at low pressures. Toyoda et al. used the molecular sieving effect of a Ca-A type zeolite with an effective diameter of 0.5 nm to adsorb N_2 but not SF_6.[10] Yamamoto and coworkers proposed a system of polymide membranes.[9] They analyzed the influence of different operating variables, such as the gas feeding pressure and the membrane temperature, on the gaseous mixture separation. Murase and coworkers selectively adsorbed SF_6 from a mixture with nitrogen by using a Na-X type zeolite with a nominal pore diameter of 1.0 nm.[11] They proposed that the filter, besides separating, could also be used as a temporary storage medium. Shiojiri et al. separated F-gases from gaseous mixtures containing N_2 by making use of the differences in surface diffusion, using a porous Vycor glass membrane.[12] Inami et al. studied the theoretical limit for SF_6/N_2 separation by liquefaction and found that the liquid SF_6 recovery efficiency decreases greatly at higher N_2 content.[8] They discussed that for SF_6 contents below 10%, even at a temperature below $-50°C$, the SF_6 recovery was almost zero.

Although available data on adsorption of pure components is widely accessible, the number of experimental studies on adsorption of mixtures is very scarce. This is mainly due to the difficulty of performing adsorption experiments with mixtures. The adsorption can be accurately determined for pure compounds by measuring the weight change of the adsorbent, whereas for mixtures additional experiments are needed to determine the composition of the adsorbate.[13] However, the development, design, and operation of separation processes by adsorption require knowledge of the physical properties of the mixture to be separated, such as the equilibrium data. A way to overcome this difficulty is by using molecular simulations in a synergetic manner with experiments: once an accurate model for the fluid and the material is found, and experimental data for the pure fluid are appropriately described, simulations of the mixture can then be used to find the optimal conditions for the separation.

The objective of this work is twofold: (1) to use molecular simulations, with simple models for the fluid and the adsorbent, as a fast way to find the optimal conditions for the separation of SF_6 from N_2, and (2) to check the validity of the results obtained with simple models with more realistic materials, searching for the best material to separate this mixture. In this work, a complementary view to the usual optimization process is given: we use molecular simulations to illustrate an optimization procedure for the separation of SF_6 and N_2 by modifying operating variables, mainly the bulk pressure and mixture composition, and atomistic level parameters, essentially the pore diameter, with the same adsorbent material. The final objective is to find the optimal pore diameter to achieve the separation by adsorption of SF_6 from a SF_6/N_2 stream. It is shown how molecular simulations can be used as a tool to optimize and design separation processes by using its predictive capabilities in a fast and reliable manner. The material used in the first stage is a cylindrical porous adsorbent, namely MCM-41. It consists of a hexagonal array of monodisperse pores formed by amorphous silica (SiO_2). This material was chosen for two main reasons: because of its simple geometry, with cylindrical pores (straightforward to be modeled with simple simulation force fields) and because of its potential as an adsorbent material for several industrial processes. MCM-41 may reach an exceptional porosity, up to 80%, making it an excellent potential adsorbent material to be used in gas storage systems, separation processes, and catalysis.[14–16] MCM-41 belongs to a family of uniform mesoporous silica materials discovered by Mobil Corporation[17,18] and it can be synthesized with narrow tunable pore size distributions, from the microporous to the mesoporous range.[19,20] Pore size tunability makes this kind of materials a good model for investigating fundamental features of adsorption such as the effects of pore size for a given geometry, and a starting point to achieve a methodical optimization.

Furthermore, the ideal smooth cylindrical pore is chosen in this work for its instructive value. Although a cylindrical pore is an overly simplistic model of real pores, it provides a useful estimate in studying the effects of confinement on selectivity. This sort of fundamental study may provide guidelines in choosing materials with the appropriate pore size for gas separation applications.[21] Throughout the first part of this article, we have chosen a simplified model of MCM-41. We have used this model to find the optimal diameter to achieve the maximum selectivity of SF_6. Simulations were later performed with more realistic materials, using atomistic models of zeolite-templated carbon materials (ZTC), chosen to assess the predictability of the results obtained with the cylindrical pore model for the optimal diameter.

ZTCs are porous carbons with a well-tailored microporous structure obtained by using the template carbonization method employing a zeolite as the template.[22,23] The pores and walls of the zeolite become the walls and pores of the carbon replica, respectively, therefore the carbon structures obtained by this method have very high-surface areas and periodic ordered structures.[24] We have chosen these templated materials in the second part of this work as a possible material for the separation of SF_6 and N_2 because, in addition to having the appropriate pore diameter, these carbon materials have good stability at high temperatures and they have a low affinity for water.[25] Besides the high mechanical properties of ZTCs make them suitable to work at high pressures.[26] These characteristics offer unique advantages over inorganic molecular sieves and make the applications of such materials very attractive. In this article, we simulated the adsorption on the pores of hexagonal (EMT) and cubic (FAU-Y) zeolite-templated carbons, which have an average pore size close to 1.1 nm.[27]

The rest of the article is organized as follows: the fluid and pore models used in the simulations are described in the following section. Next, we give the essential information on the simulation method used for computing the adsorption behavior. Then, we show the influence of the diameter on the separation process of sulfur hexafluoride, and find the optimal diameter for selecting SF_6 over N_2. Besides, we discuss the effect of using two different kinds of models for the fluid molecules on the simulation results. Then the results for the optimal diameter for the separation are contrasted with a more realistic material by using two model Zeolite-Templated Carbons.

Models

Fluid models

We have considered two sets of models for each fluid molecule. The first one consisted of simple 1-site Lennard-Jones (LJ) model, which means representing the fluid molecules by spheres with van der Waals type attractive and repulsive interactions; this set of models was used for the initial stage of the optimization procedure. Although predictions from these models are usually less accurate than those obtained with more refined force fields, the 1-site model requires less computational resources while providing a first good approximation for the appropriate separation conditions. This set of models was used to run a series of adsorption isotherms with a broad range of pore diameters and a smaller separation step between each diameter. The results obtained from the 1-site model were further refined by using a second set of models, in which we introduced more degrees of freedom to the molecular structure to get more realistic predictions. For this second set, we have used a flexible 6-site model for sulfur hexafluoride developed by Olivet and Vega.[28] and a 2-site model for nitrogen developed by Galassi and Tildesley.[29] The values of the LJ parameters for each model are provided in Table 1.

Several LJ parameters for 1-site SF_6 and N_2 models are available in the literature.[30,31] Some of them have been adjusted to predict the vapor–liquid coexistence region, while others are more accurate for the estimation of transport properties. In this work, the parameters for the LJ potential for both molecules were obtained by adjusting the experimental vapor–liquid equilibrium densities using the soft-SAFT equation of state, using just the reference term of this equation, which is a LJ spherical fluid.[32,33] The advantage of using this procedure is that the equation is very accurate for these fluids, and in addition, it provides a straightforward relationship between the pressure and the chemical potential, needed for the adsorption isotherms.

Table 1. Lennard-Jones Parameters for the Simulated Force Fields for N_2 and SF_6 Used in This Work

Force Field	σ (Å)	ε/k_b (K)
1-site SF_6	4.650	251.1
Multisite flexible SF_6 (six F)	2.769	73.13
1-site	3.582	98.83
Multisite N_2 (2 N)	3.310	93.98

Note that in addition to these values, additional parameters are used for the bonds and angles for the multisite models. See text for details.

In the 1-site model, the interaction energy, U_{inter}, between two molecules i and j, is accounted for by the Lennard-Jones potential.

For multisite models, the SF_6 molecule is represented by different interacting sites. The total intermolecular interaction between two molecules is calculated as the sum of the energies of point-site interactions in each molecule. The model used for SF_6 explicitly includes the flexibility of the molecule; thus, the intramolecular energy for one molecule, U_{intra}, is calculated as a sum of the equilibrium bond and equilibrium angle energies.

$$U_{intra} = \sum_{bonds} K_r(r_{ab} - r_0)^2 + \sum_{angles} K_\theta(\theta_{ABC} - \theta_0)^2 \qquad (1)$$

K_r and K_θ are the force constants for the bonds and angles, respectively. r_{ab} is the distance between atoms a and b, and r_0 is the equilibrium distance for that pair of atoms. θ_{ABC} is the angle formed by the atoms A, B, and C, whereas θ_0 is their equilibrium angle.

The multisite model used in this work for SF_6 was the flexible force field proposed by Olivet and Vega.[28] In this model, explicit interactions are only considered to occur among fluorine atoms. All interactions involving sulfur atoms are neglected on the assumption that a modified fluorine-fluorine LJ potential could incorporate any sulfur-sulfur or sulfur–fluorine interactions. To account for the flexibility of the molecule, this model uses six harmonic stretching terms for modeling the S-F bonds and twelve harmonic bending terms for modeling the F-S-F angular deformations. This force field was obtained by simultaneously fitting selected vapor–liquid equilibrium (VLE) and transport properties to available experimental data and it has proven to give excellent results for transport properties of SF_6/N_2 mixtures.[34] The values of the parameters for the flexible part of this potential are $\theta_0 = 90°$, $K_\theta = 307.36$ kJ/mol rad^2, $r_0 = 0.1565$ nm and $K_r = 69348.0$ kJ/mol nm^2.

To represent the diatomic N_2 molecule, we used the model proposed by Galassi and Tildesley.[29] This force field uses a

rigid dumbbell representation for N_2 molecules, with a distance between the nitrogen atoms of 0.1089 nm, and the intermolecular interactions are quantified by a LJ potential. The parameters of this potential were fitted to reproduce experimental VLE data.

Solid adsorbents

As mentioned in the introduction, the adsorbent material used in the simulations for finding the optimal diameter was first a porous silica material, MCM-41, and later two Zeolite-Templated Carbons (ZTC).

MCM-41 was represented by a simple cylindrical model, taking the potential form given by Tjatjopoulos.[35] This model assumes that the regular hexagonal surface of MCM-41 can be represented by a cylindrical homogeneous surface, in which the interaction sites are continuously distributed on a sequence of concentric surfaces that compose the pore wall.

$$U_{\text{wall}}(r,R) = \pi^2 \rho_s \varepsilon_{\text{sf}} \left[\begin{array}{l} \frac{63}{32}\left[\frac{r}{\sigma_{\text{SF}}}\left(2-\frac{r}{R}\right)\right]^{-10} F\left[-\frac{9}{2};-\frac{9}{2};1;\left(1-\frac{r}{R}\right)^2\right] \\ -3\left[\frac{r}{\sigma_{\text{SF}}}\left(2-\frac{r}{R}\right)\right]^{-4} F\left[-\frac{3}{2};-\frac{3}{2};1;\left(1-\frac{r}{R}\right)^2\right] \end{array} \right] \quad (2)$$

The variables R and r represent, respectively, the effective radius of the cylindrical pore and the distance between the interaction points of the fluid and the wall. The function $F[a;\ l;\ x;\ c]$ denotes the hypergeometric series. The values for the solid parameters used in this work were taken from Ravikovitch et al., $\rho_S = 15.3\ \text{nm}^{-2}$, $\varepsilon_S/k_B = 193.1$ K and $\sigma_S = 0.2725$ nm.[36]

The simple surface potential of Tjatjopoulos et al. is considered an appropriate choice to show the suitability of molecular simulations to be used as a tool in process design. The use of this potential for the solid surface avoids additional complexity in the simulated system and saves computational time. Previous works have reported accurate results when using this potential for predicting adsorption isotherms as compared to experimental systems.[36–41]

The atomistic models employed in the simulations for more realistic materials represent two ordered microporous carbon replicas of siliceous forms of faujasite zeolite (cubic Y-FAU and hexagonal EMT). These atomistic models for ZTC were proposed by Roussel et al.[42] Simulations of adsorption isotherms for characterizing ZTC using those models materials have been reported previously.[42,43] The ZTC structures were assumed rigid and the parameters for the carbon atoms in the ZTC were taken to be those customarily used to describe the carbon atoms of graphene sheets, $\varepsilon_C = 28.0$ K and $\sigma_C = 0.34$ nm.[44]

Simulation Details

The simulation of the adsorption process was done using Grand Canonical Monte Carlo (GCMC) simulations. As this is a standard procedure for molecular simulations of adsorption, the reader is referred to a reference book on the subject[45] for details on the simulation procedure, retaining here just the main details concerning the implementation for the particular systems of interest.

The GCMC simulations for the cylindrical pore were done employing: (1) a simulation cell consisting of a cylinder with a diameter ranging from 1.0 to 4.0 nm and a fixed length of 10.0 nm, (2) a cutoff radius of at least 6 times the collision diameter of the fluid molecules (σ_{LJ}),[46] (3) 1.5×10^5 MC steps for equilibrating the system and 2.0×10^6 MC steps for data collection, (4) an equal a priori probability to displace, insert or remove a molecule in each simulation step and (5) periodic boundary conditions in the z-direction. The parameters ε_{ij} and σ_{ij} were calculated from their homoatomic pairs according to the Lorentz Berthelot combining rules.

Experimentally, the pressure of a gas reservoir is imposed on the adsorption system. As the simulations in the confined system are done at fixed chemical potential, comparisons between the results of molecular simulations and experiments require an explicit relationship between the pressure, P, (or the fugacity) of the reservoir and its chemical potential, which can be provided by any accurate equation of state or calculated by simulations of the same force field. In this work, the chemical potential was related to the pressure and the composition in the reservoir by means of the soft-SAFT equation of state, used as an accurate LJ equation of state, fitted to simulation data. For consistency, we fitted the VLE diagrams of each model using the soft-SAFT equation, obtaining slightly different parameters depending on the models; these tuned parameters were used to calculate the chemical potential at different pressures. Although we have used soft-SAFT for this purpose, any other accurate equation of state for these two fluids could be used to relate the pressure to the chemical potential.

The simulation conditions were chosen to mimic the experimental conditions at which this separation takes place. For the thermodynamic conditions, we have used the following values: the compositions for the fluid in the reservoir comprised a serie of values from pure SF_6 to pure N_2, which in terms of SF_6 mole fractions were 0.00, 0.10, 0.25, 0.50, 0.75, 0.90, and 1.00; these values account for the entire composition range. The pressure in the reservoir ranged from 50 to 2000 kPa, we chose this maximum value of pressure, a value below the saturation pressure of pure SF_6, in order to compare the advantages of using adsorption over conventional liquefaction, and as the minimum pressure we used a value close to the atmospheric. Finally, the temperature of the reservoir was fixed at 300 K to simulate adsorption at room temperature.

The simulations of the ZTCs were run at the same thermodynamic conditions than the MCM-41 simulations, except that only two selected representative conditions for the mixture were simulated for the mixture composition: an bulk equimolar mixture of SF_6/N_2, and a mixture with low contents of SF_6 (0.1 mole fraction), as well as both pure fluids. The GCMC simulations were performed on a periodic box containing a unit cell of cubic FAU-ZTC (2.485 nm) and for a hexagonal EMT-ZTC (corresponding to two hexagonal orthorhombic unit cells in x,y directions: $a = 3.4772$ nm, $b = 3.0114$ nm, and $c = 2.8346$ nm). The systems were equilibrated for 1.0×10^6 Monte Carlo steps and 4.0×10^6

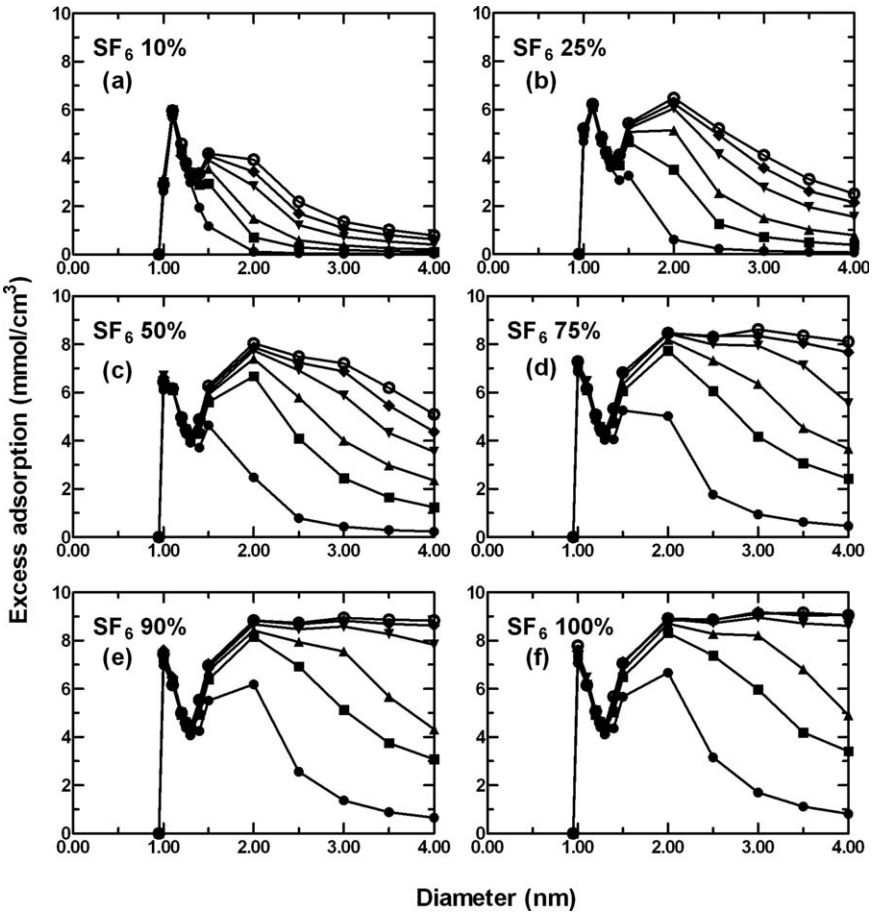

Figure 1. SF_6 excess adsorption isotherms for mixtures of SF_6 and N_2 using a 1-site model. See text for details.

For pressures of 50 kPa (filled circles), 250 kPa (squares) 500 kPa (upward triangles), 1000 kPa (downward triangles), 1500 kPa (rhombs), and 2000 kPa (open circles).

Monte Carlo steps were further performed for averaging purposes. The cut-off radius was taken to be less than half the simulation box length.

Results

We present next the most relevant results divided in three parts: first, the separation of SF_6 from N_2 in MCM-41 considering 1-site models for the fluid and a wide range of pore diameters, pressures, and compositions; second, the separation of the same mixture in the same material at the optimal conditions found in the first case, but considering multisite models for the fluids; and, finally, the separation of the mixture using an atomistic model for the solid.

Separation considering one-site models for the fluids

We present next the adsorption isotherms and the selectivity of MCM-41 for SF_6 and N_2, modeled as a 1-site LJ spheres, using a range of pore diameters from 1.0 nm to 4.0 nm. The results of the GCMC calculations are plotted as excess isotherms (or excess pore density), in order to include only the amount of gas that is adsorbed due to the pore walls. The excess pore density, ρ_{exc}, is the difference between the absolute density in the pore and the bulk gas density; the absolute density can be defined as the ensemble average of the number of particles per unit of accessible volume.

$$\langle \rho_{exc} \rangle = \frac{\langle N \rangle}{V} - \rho_{bulk} \tag{3}$$

The mean number of molecules inside the pore, $<N>$, is computed from the GCMC simulations and ρ_{bulk} is the bulk density obtained from the equation of state.

The excess adsorption isotherms for SF_6 at different pore sizes and compositions of the reservoir are shown in Figure 1 (ranging from 1a to 1f, as a function of the mixture composition). The plots show the change in the adsorption behavior going from a diluted gas mixture, 0.1 mole fraction of SF_6 in Figure 1a, to pure SF_6, in Figure 1f.

Two important characteristics of the adsorption behavior can be extracted from the SF_6 adsorption isotherms. First, there is an inflection point at a pore diameter of 2.0 nm: the effect of the composition on the adsorption of SF_6 behaves differently above and below this size. For pore diameters

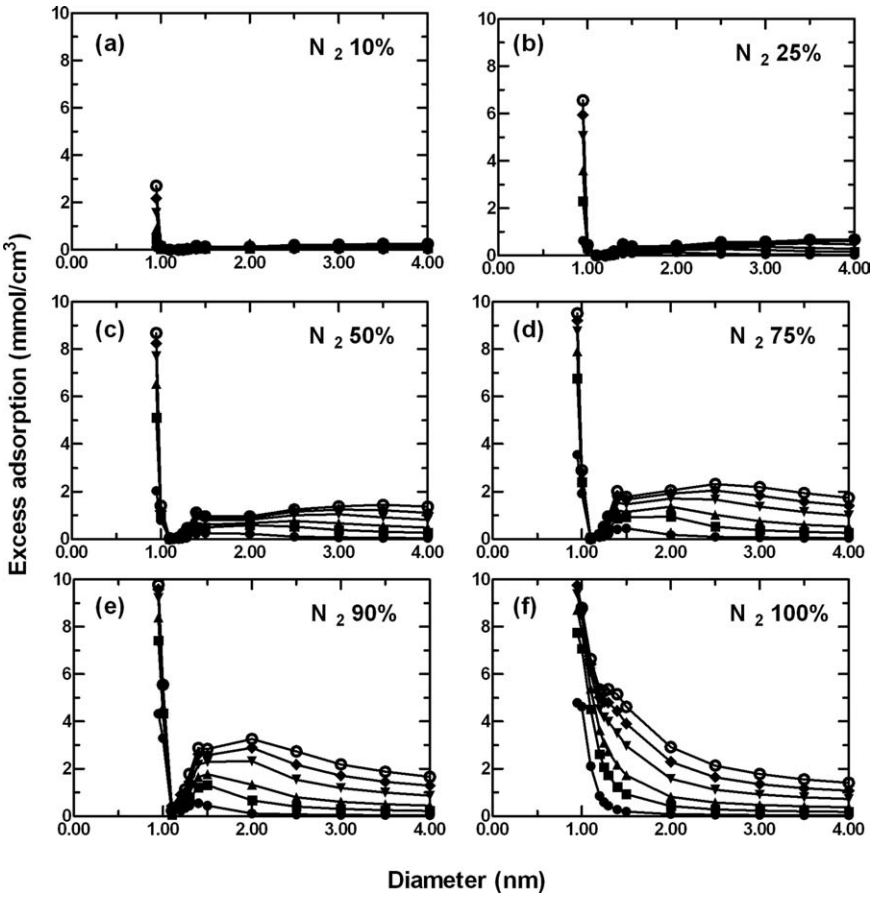

Figure 2. N_2 excess adsorption isotherms for mixtures of SF_6 and N_2 using a 1-site model.

Symbols as in Figure 1.

smaller than 2.0 nm the amount of SF_6 adsorbed is a weak function of the composition. Even at low molar fractions of SF_6, its behavior is similar to pure SF_6. Moreover, for larger pore sizes, it diminishes when the concentration of N_2 in the bulk increases. This indicates that SF_6 is strongly attracted towards the wall. The fluid–solid interactions weaken when the loading increases, as more molecules are forced to remain in the center of the pore, where the attraction due to the walls is smaller.[47] The second characteristic is, that for all the diameters studied, a pressure of 2000 kPa saturates the pore with pure SF_6, see Figure 1f. Hence, the point of maximum adsorption, which is an indication of the capacity of the solid material, is reached at low pressures. The 1-site model for SF_6 predicts that the fluid-wall interactions are very strong and the pores are filled up at low pressures. This is also seen in the excess isotherm plots at SF_6 mole fractions above 0.75, Figures 1d–f, which are almost equal; at high contents of SF_6 the isotherms behave almost as if it was pure SF_6. This is a typical behavior for the larger molecule in the adsorption of binary mixtures: at the lowest relative pressures, the larger molecule is strongly attracted to the wall and it saturates the pore faster than the smaller molecule.[48,49]

The excess adsorption isotherms for N_2 at different pore sizes and initial bulk compositions are depicted in Figure 2. The adsorption isotherms of N_2 show a strong influence of the composition on the adsorbed amount, this might be due to the SF_6 molecules being more attracted towards the wall and blocking the space for N_2 adsorption. For pore diameters larger than 2.0 nm the adsorption of N_2 is very low for the pressure range analyzed. For a pore size of 1.0 nm, N_2 is strongly adsorbed, due to the confinement, when the mole fraction of SF_6 is small; once SF_6 concentration starts to increase, the adsorbed amount of N_2 diminishes abruptly. This sudden decline of N_2 adsorption is due to the larger SF_6 molecule entering the small pore occupying almost all the free space, making it harder for the N_2 molecules to adsorb. The lessening of N_2 adsorption with increasing content of SF_6 weakens at larger pore diameters. This might be due to the fact that the adsorbed SF_6 molecules near the solid wall create an attractive energy that facilitates adsorption of N_2, e.g., for a diameter of 4.0 nm the adsorbed amount of N_2 with 0.25 mole fraction of SF_6 is higher than it is for pure N_2.

An advantage of using molecular simulations is the additional microscopic information provided by them, as one is able to locate the molecules in their equilibrium configurations, as shown in Figure 3 for different pore diameters. The adsorption isotherms illustrate that at 1.1 nm the amount of adsorbed N_2 is negligible. As observed in Figure 3b, the exclusion of N_2 in the pore of 1.1 nm is due to the SF_6

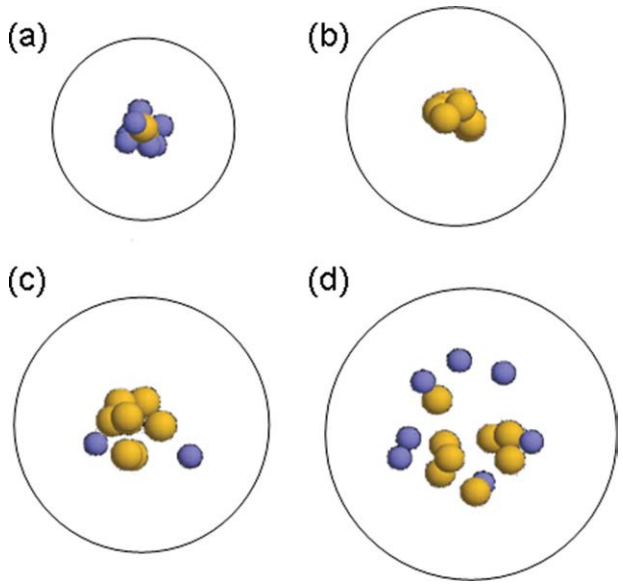

Figure 3. Snapshots of adsorbed SF_6 and N_2 at different pore sizes for mixtures with a molar fraction of SF_6 of 0.10.

Pore diameters (a) 1.0 nm, (b) 1.1 nm, (c) 1.2 nm, and (d) 1.3 nm. SF_6 is represented in yellow and N_2 is represented in blue. [Color figure can be viewed in the online issue, which is available at wileyonlinelibrary.com.]

molecules, more strongly attracted toward the solid, accommodated in an alternating fashion. At smaller pore diameters (see Figure 3a) SF_6 accommodates in a straight line because of the strong effect of the pore walls, and N_2 molecules can distribute around the SF_6 molecules. Although for pore diameters larger than 1.1 nm (see Figures 3c, d) the SF_6 is distributed in a similar way but these larger pore sizes allow enough free space for N_2 to adsorb. Hence, for the 1.1-nm pore the SF_6 molecules distribute in such a way that the free space among SF_6 molecules and the solid walls is not large enough for N_2 molecules to fit, thus SF_6 selectively adsorbs, excluding almost completely, the N_2 molecules. This exclusion of the smaller molecule was first predicted by Sommers et al., for two spherical particles of different sizes in slit pores.[50] This effect is more pronounced due to the simple geometry of the force fields, modeling the molecules as spheres, thus they are not allowed to rotate and find free space within the pore to be adsorbed.

Regarding the separation of the mixture as a function of composition, Figure 2 shows that for SF_6 mole fractions above 50% the amount of N_2 adsorbed is very small, thus it is a simple task to separate an enriched mixture of SF_6 with N_2, as pointed out by Inami et al.[8] They claimed that this enriched mixture could be separated by compressing and cooling the gas. The advantage of using adsorption, as done

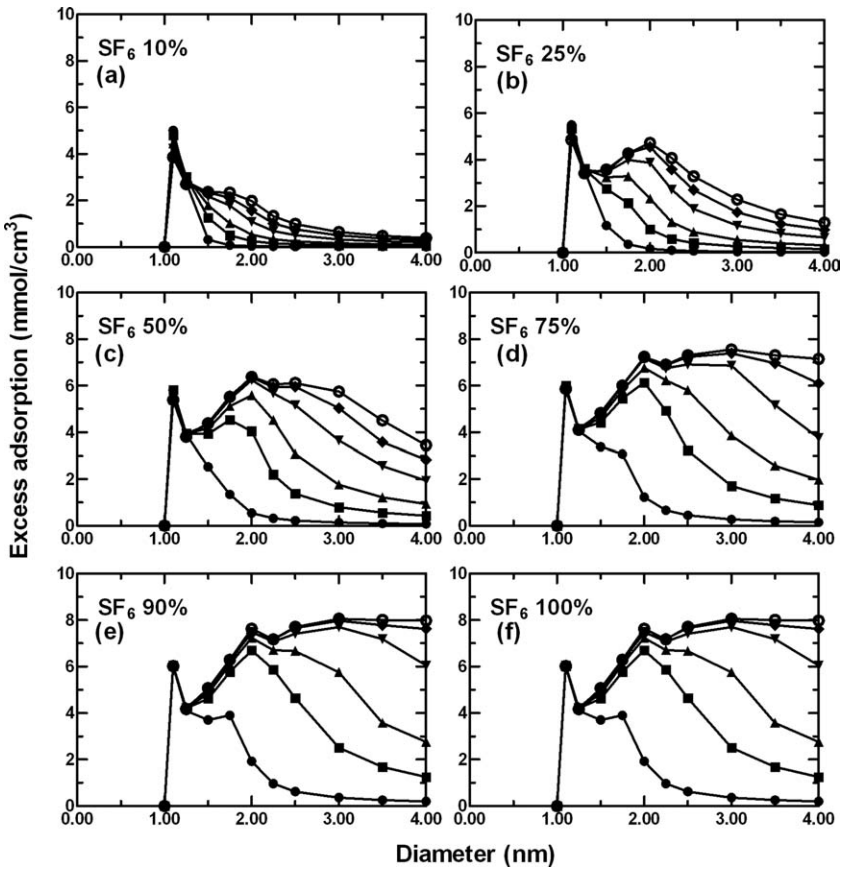

Figure 4. SF_6 excess adsorption isotherms for mixtures of SF_6 and N_2 using multisite models for the fluids. See text for details.

Symbols as in Figure 1.

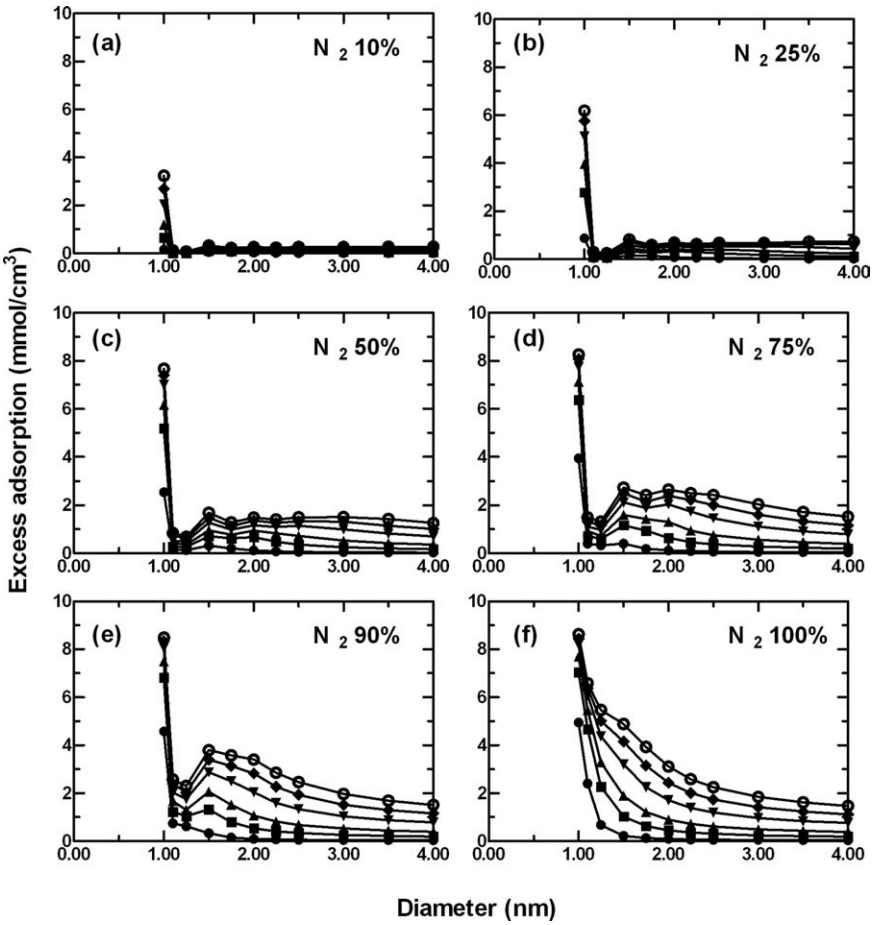

Figure 5. N_2 excess adsorption isotherms for mixtures of SF_6 and N_2 using multisite models for the fluids.

Symbols as in Figure 1.

in this work, is that using an adsorbent, as shown here, overcomes the difficulty of recovering SF_6 from the gas mixture lies in the separation of SF_6 from diluted mixtures, once the proper diameter for effective separation is found.

At higher pressures, N_2 starts to adsorb in the pore and begins to displace SF_6, compared to the adsorption of pure SF_6. This competitive adsorption effect has been observed in other binary mixtures, such as the mixture of CO_2 and N_2 in metal–organic frameworks, where CO_2 is preferentially adsorbed at low pressures but it is displaced by N_2 at higher pressures.[51] For instance, for a SF_6 molar fraction of 0.1, the amount of SF_6 adsorbed at 1.5 nm reaches a plateau before 1000 kPa, further increasing the pressure only increases the adsorbed amount of N_2. This competitive behavior is due to the nonideal behavior of SF_6 at higher pressures, as at these conditions the fugacity of SF_6 starts to deviate from the ideal behavior, while N_2 acts almost as an ideal gas. Thus, the fugacity of SF_6 does not increase as steeply with pressure as it does for N_2; therefore it becomes increasingly easier to adsorb N_2 molecules as the acceptance rule for the creation of new molecules directly depends on the fugacity.[52]

The selectivity is the preference of one substance over the other (or others) in the mixture to stay in a given phase; for adsorption processes, it is desirable to have a high selectivity of the substance to be separated. For SF_6 and N_2 in any adsorbent the selectivity is defined as:

$$S_{SF_6-N_2} = \frac{x_{SF_6}/x_{N_2}}{y_{SF_6}/y_{N_2}} \tag{4}$$

The selectivity of SF_6 over N_2 is $S_{SF6\text{-}N2}$, where x_{SF6} and x_{N2} are the mole fractions of the two components on the adsorbent surface; y_{SF6} and y_{N2} are the corresponding mole fractions in the bulk. Values of selectivity larger than one mean that SF_6 is preferentially adsorbed over N_2.

According to Babarao et al. simulations are useful for estimating the general trend of the selectivity, but its value cannot be accurately assessed solely from molecular simulations, as small deviations in the number of molecules might result in a large change in the selectivity.[53] The results of the selectivity using the 1-site model do not present meaningful information in this case, as the complete exclusion of the N_2 molecules for a pore diameter of 1.1 nm makes the selectivity for that pore diameter to tend to infinity. However, for an adsorbent it is important to have both high adsorption capacity and selectivity. The adsorption capacity for a pore diameter of 1.1 nm is among the highest for the pressure range analyzed, and due to the exclusion of N_2 at

this pore size the MCM-41 adsorbent is highly selective toward the adsorption of SF_6.

To assess the reliability of these results from molecular simulations we have further investigated this case (pore diameter of 1.1 nm) , using a more refined force field for the fluid, which takes into account details of the molecular structure of the molecules, expecting that this should have an effect on the adsorption. Results are presented in the next subsection.

Separation considering multisite models for the fluids

Once a throughout study with the optimal conditions for separation was performed with simple models, we have carried out additional simulations using multisite models to confirm the results and test the reliability of the 1-site model for optimizing process equipment for these mixtures and material. Of special interest to the present study is the pore diameter close to 1.1 nm, given the results obtained for the 1-site model.

As aforementioned in the model section, multisite models have additional degrees of freedom with respect to the 1-site model: multisite molecules can change their orientation and, in the case of flexible models, the bonds and angles can vibrate. SF_6 is a highly symmetric molecule that can be represented by a spherical model, with either 1-site or multisite. Whereas N_2 is a linear molecule; it has been discussed the problems in interpretation and predictions resulting of using a 1-site model for a linear molecule.[54,55] The introduction of these changes in the molecular models has a significant effect on the adsorption behavior of pure components, especially at diameters where the adsorption begins its transition from monolayer to multilayer.[54] As the simulations for the 1-site models gave an optimal adsorption diameter of 1.1 nm, this diameter lies within this transition range[56] and it is worthy further investigating it with the more refined fluid models. It is expected that the results differ from those obtained with the 1-site spherical LJ models mainly because of the nature of N_2, but also because of the additional details introduced for the SF_6 molecule.

The adsorbed amount of SF_6 predicted by the multisite models is depicted in Figure 4. The most noticeable characteristic of these plots, compared to Figure 1, is the lack of adsorption of SF_6 at 1.0 nm; SF_6 molecules of the multisite model cannot fit in the 1.0 nm pores. This behavior is also seen in the 1-site models for a pore diameter of 0.95 nm.

The maximum capacity, for the pressure range studied, is reached for a pore diameter of 2.0 nm, as observed for the 1-site model. The main difference between Figures 1 and 4 is the total amount of SF_6 adsorbed in the material; it is smaller for the multisite model than for the 1-site one, especially at low SF_6 molar fractions. Another important difference between the two sets of results is the slope of the isotherms. The 1-site model has a steeper slope than the multisite one, due to the differences in the geometry of the molecules.

The adsorbed amount of N_2 predicted with the multisite models is depicted in Figure 5. The adsorption of N_2 molecules obtained when using the multisite model is not as affected by the presence of SF_6 molecules as it was for the 1-site model, hence, the decrease in the adsorption of N_2 with the presence of SF_6 molecules is less marked. Additional insights into this effect can be inferred by looking at the equilibrated configurations, shown on Figure 6. In the 1.0-nm pore, only N_2 molecules can get inside the pore and SF_6 molecules are excluded, as seen in Figure 6a. Figure 6b shows the local minimum for the adsorption of N_2 observed at 1.1 nm. SF_6 molecules block a large portion of the free volume for the adsorption of N_2, although in this case, because of the linear geometry 2-site model, N_2 molecules can rotate and accommodate to find free space in the narrow pore.

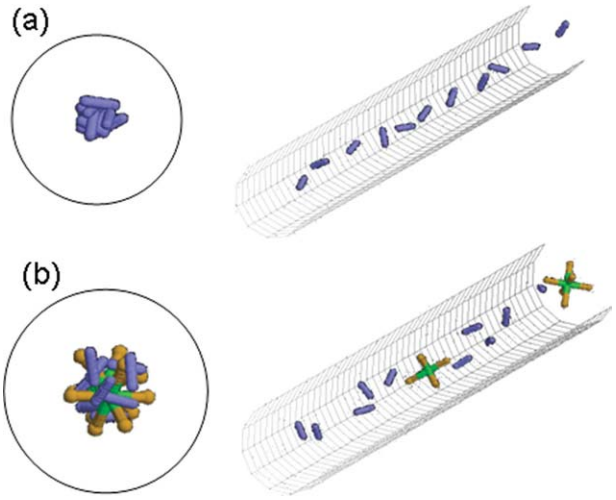

Figure 6. Snapshots of adsorbed SF_6 and N_2 at different pore sizes with a molar fraction of SF_6 of 0.10.

Pore diameters (a) 1.0 nm and (b) 1.1 nm. N_2 is represented in blue while SF_6 is represented in yellow (the F atoms) and green (the bonds between atoms). [Color figure can be viewed in the online issue, which is available at wileyonlinelibrary.com.]

The competitive adsorption of N_2 at higher pressures is seen better for the multisite models than for the LJ model, partially due to the fact that the amount of adsorbed SF_6 is lower in this case, and also because the linear N_2 molecules pack more easily near the pore wall, being able to adsorb more than the spherical ones at lower pressures.

The local minimum observed in the N_2 adsorption for a pore diameter of 1.1 nm (for molar fractions of N_2 below 0.75) is also reflected in the selectivity plots shown in Figure 7; the maximum selectivity is reached at this point of minimum N_2 adsorption. This optimum selectivity occurs at a pore size where SF_6 blocks the free space for the adsorption of N_2, enhancing the separation of their molecules. This effect diminishes with pressure, because the higher pressures favors the competition between SF_6 and N_2 and also the packing of the molecules increases, creating more small accessible free spaces.[57] Furthermore, the minimum adsorption (a local minimum) for SF_6 is found at 1.5 nm, which is reflected in the selectivity plot as the minimum in selectivity. This selectivity minimum is the point where the transition from a single to multiple layers of SF_6 is achieved.

The selectivity follows the trend predicted by the theoretical analysis in a one-dimensional system performed by Talbot.[48] The larger molecule is attracted in a stronger manner

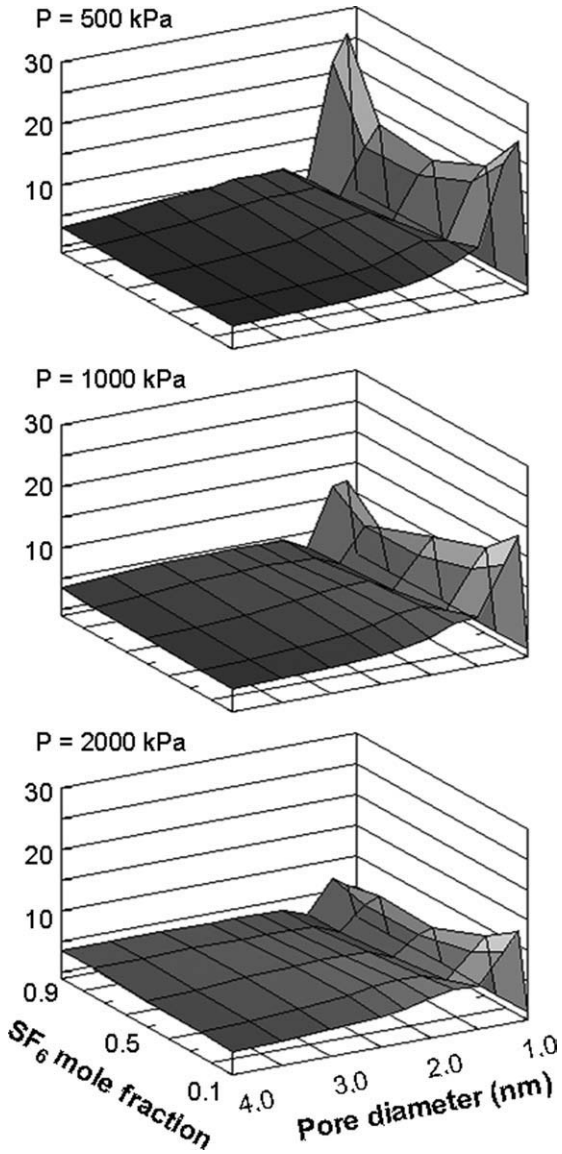

Figure 7. Selectivity of SF_6 over N_2 using multisite models.

to the solid material. For pressures below the iso-selective point the composition has a strong influence on the selectivity, while when approaching the isoselective point, increasing the pressure reduces the differences among the different compositions. It is also worth noting that a decrease of the selectivity with pressure for all compositions is achieved due to the competitive adsorption already discussed. At low pressures (see Figure 7a), the material is more selective towards SF_6 than at higher pressures, because a competitive adsorption with N_2 that takes place at higher pressures.

Finally, in a similar fashion to the 1-site model, the selectivity is independent of pore size and composition for pores wider than 2.0 nm, due to the free volume available for both molecules to adsorb, whereas the selectivity decreases with pressure, because of the competitive adsorption and the packing effect of N_2. This independency of selectivity with pressure has been observed for other solid adsorbents with large pore sizes and high volumetric capacity, such as a mixture of CH_4/H_2 in non-interpenetrated MOFs.[47,58]

Separation using an atomistic model for the solid

As a final step in this study, once the optimal conditions for separation were found with the simple models, and these conditions corroborated with the refined force fields for the fluid, we have checked the performance of a realistic material with a pore diameter similar to the one found for optimal separation, to check its performance for separating this mixture. For this purpose, we have used two different solid materials with different shapes and similar pore sizes: (1) FAU-ZTC, which has a sharp pore size distribution located around 1.1–1.2 nm, and (2) EMT-ZTC, which has a bimodal and wider pore size distribution around 0.8-1.1 nm.[27,42] Snapshots of both structures are presented in Figure 8 while details on the materials can be found in the original references.[27,42]

Although the values for the adsorption isotherms should be different from those of the silica cylindrical model, ordered materials with almost cylindrical structures, such as zeolites or zeolite carbon replicas, should follow the general trend observed with the ideal cylindrical pore.

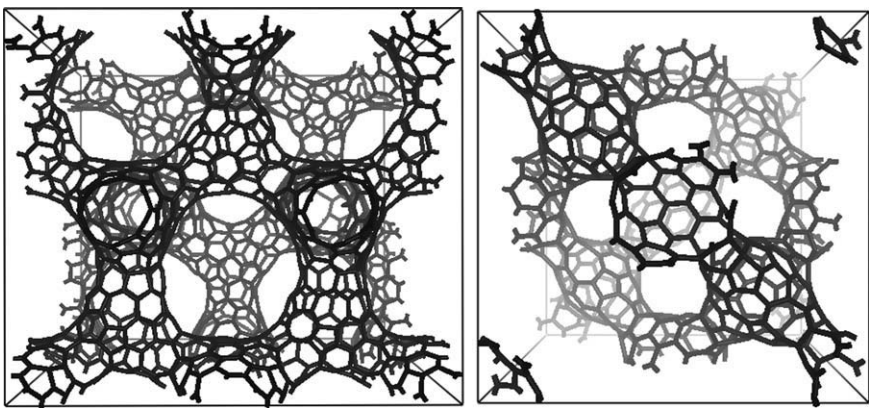

Figure 8. Models of the atomistic structures: EMT-ZTC (left) and FAU-ZTC (right).

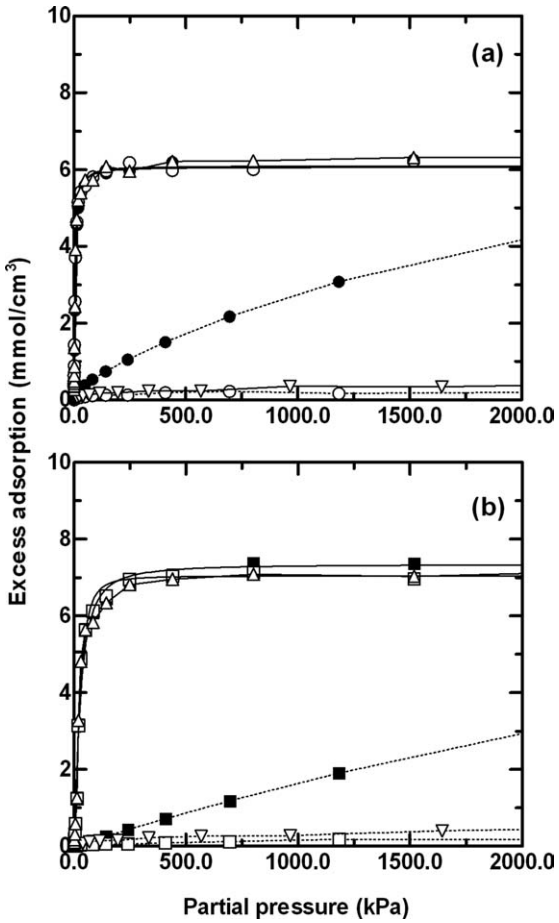

Figure 9. Adsorption isotherms of pure SF_6, pure N_2 (closed symbols, full, and dashed line respectively), SF_6, and N_2 in an equimolar mixture in the bulk (open symbols, full and dashes line respectively), and SF_6 and N_2 in a mixture with 0.1 molar fraction of SF_6 (upward and downward triangles, respectively) on EMT-ZTC (a) and FAU-ZTC (b) as function of the partial pressure of each fluid.

The adsorption isotherms of SF_6 and N_2 on ZTC materials, as a function of the partial pressure of each substance, are depicted in Figure 9. It can be observed in the figure how N_2 is displaced by SF_6 during the adsorption on both EMT-ZTC (Figure 9a) and FAU-ZTC (Figure 9b). The adsorption isotherms for pure SF_6 are almost identical to the isotherms of SF_6 in the mixture, whereas for N_2 the adsorption isotherms of the pure fluid are far higher than when SF_6 is present. The amount of SF_6 adsorbed on FAU-ZTC (the material with a sharp pore size distribution at the desired pore size) is higher than for EMT-ZTC, and the opposite behavior is observed for N_2. This behavior means excellent efficiency for the separation on FAU-ZTC, as confirmed by the selectivity plots depicted in Figure 10. For pressures between 100 and 1000 kPa on FAU-ZTC an optimal separation efficiency is achieved, with selectivity values around 130, much higher than any other previously reported material for this mixture separation.

The slope of the adsorption isotherms is steeper for EMT-ZTC; this means that the solid–fluid interactions are stronger in this material. This is reflected in the selectivity, which decreases with increasing pressure for EMT-ZTC, while for FAU-ZTC the selectivity first increases until a certain pressure, and then it begins to decrease with pressure; at this point, the total capacity for SF_6 adsorption has been reached and the competitive adsorption of N_2 begins to displace some SF_6.

The predictions of the optimal diameter show that FAU-ZTC is an excellent technical option for separating SF_6/N_2 mixtures. This can be seen by comparing the values of the selectivity for FAU-ZTC (and even EMT-ZTC) to the ones reported in the literature. Experimentally, for inlet compositions of 0.10 mole fraction of SF_6 on a Ca-A zeolite a selectivity of 28.5 was obtained,[10] likewise a selectivity of 44.3 on a Na-X type zeolite[11] and a selectivity of 12.8 was obtained on Vycor glass.[12] In addition, the best adsorbent material in terms of selectivity, found in the literature (Na-X zeolite) has an average pore size of 1.0 nm. This confirms the results of our simulations, with the cylindrical model, for the optimal pore diameter. It is important to note that the values reported in the literature are equivalent to a dynamical separation process, whereas the values reported here are equivalent to a fixed value at a certain composition. We report the values of our simulations for a molar fraction of SF_6 of 0.5 to take into account this difference. At low SF_6 concentration in the bulk, the selectivity is even greater.

Given the comparison with the other materials for SF_6/N_2 separations, the carbon replicas used here show a very promising capability for separating SF_6/N_2 mixtures from a practical point of view, especially FAU-ZTC. The mechanical properties of ZTC would allow the separation using a device as the one portrayed by Murase et al.[11] as a way feasible to separate and store SF_6 for its recovery and reutilization.

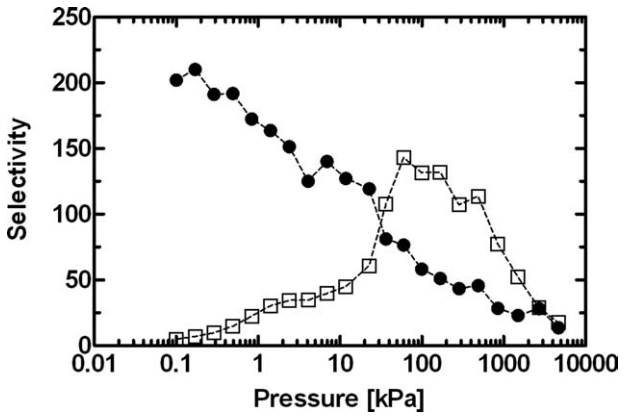

Figure 10. Selectivity of SF_6 over N_2 on EMT-ZTC (circles) and FAU-ZTC (squares) for a bulk equimolar mixture.

Conclusions

This study illustrates how molecular simulations can be used to guide the selection for the optimal conditions for separations of mixtures by adsorption, and how an optimal material can be found following this procedure. The methodology has been applied to separate, by adsorption, sulfur hexafluoride (SF_6) from nitrogen (N_2), a mixture of key interest for electrical applications, and a separation needed to avoid the emission of SF_6 into the atmosphere.

We have first studied the influence of composition, pressure and pore diameter on the adsorption and separation of SF_6 and N_2 mixtures in MCM-41 by using GCMC molecular simulation as a way to optimize the separation process. Results show that the maximum selectivity by adsorption is obtained for a cylindrical pore diameter of 1.1 nm; where sulfur hexafluoride molecules block the empty volume of the pore and prevent nitrogen from being adsorbed. The importance of using molecular simulation to find the optimum value is clearly shown by the narrow range of pore diameters with high selectivities; in addition, simulations help to visualize the distribution and orientation of the molecules at the molecular level. It has been obtained that the selectivity is almost independent of the pore diameter and the mixture composition for pore diameters larger than 2.0 nm, due to the free available volume for the two components. Further simulations with more refined force fields for the fluids, including geometrical information and flexibility of the molecules, mainly corroborate the optimal conditions for separation obtained with the simple models.

Once the optimal pore diameter for separation in the simple MCM-41 model material was found, additional simulations were performed in ordered materials with almost cylindrical structures, such as zeolite carbon replicas (Zeolite Templated Carbons, ZTC). GCMC simulation results show very high selectivities for FAU-ZTC and EMT, being the selectivity higher for FAU-ZTC, a material with a narrow pore size distribution located around 1.1 nm. Selectivities found for this material are approximately four times higher than the best material for separation published in the open literature. Given the mechanical properties of these carbon replicas, these materials show a great potential for applications in recovering SF_6 from SF_6/N_2 mixtures present in gas-insulated equipment.

Acknowledgments

The authors acknowledge the contributions from A. Olivet to early stages of this work. They are also grateful to J.S. Andreu for discussions and for providing the soft-SAFT calculations used in this work. Contributions from R.J-M Pellenq and C. Bichara related to the ZTC materials are also gratefully acknowledged. The computational time provided by CESCA, the supercomputer Center of Catalonia is deeply appreciated. Financial support has been provided by the Spanish Government, through projects CTQ2008-05370/PPQ, NANOSELECT and CENIT SOST-CO2 (CEN-2008-1027), the last two projects belonging to the Programa Ingenio 2010. Additional support from the Catalan Government was also provided (2009SGR-666). S.B. acknowledges a grant from MATGAS 2000 AIE.

Literature Cited

1. Kyoto Protocol to the United Nations Framework Convention on Climate Change. RECIEL. Volume 7 Issue 2, pp. 214–217 (http://dx.doi.org/10.1111/1467-9388.00150).
2. Ravishankara AR, Solomon S, Turnipseed AA, Warren RF. Atmospheric lifetimes of long-lived Halogenated species. *Science*. 1993; 259:194–199.
3. Etter M, Koch H. Sulfur hexafluoride SF6. Paper presented at Power and Energy Society General Meeting-Conversion and Delivery of Electrical Energy in the 21st Century, 2008, IEEE 2008. Available at: http://dx.doi.org/10.1109/PES.2008.4596619.
4. Olthoff JK, Christophorou LG. A brief history of gaseous dielectrics research at NIST. Paper presented at Electrical Insulation and Dielectric Phenomena, 2001 Annual Report. Conference on 2001. Available at: http:/dx.doi.org/10.1109/CEIDP.2001.963539.
5. Hikita M, Ohtsuka S, Okabe S, Kaneko S. Insulation characteristics of gas mixtures including perfluorocarbon gas. *IEEE Trans Dielectric Electric Insul*. 2008;15:1015–1022.
6. Katagiri H, Kasuya H, Mizoguchi H, Yanabu S. Investigation of the performance of CF3 gas as a possible substitute for SF6. *IEEE Trans Dielectric Electric Insul*. 2008;15:1424–1429.
7. Taniguchi S, Okabe S, Takahashi T, Shindo T. Discharge characteristics of 5 m long air gap under foggy conditions with lightning shielding of transmission line. *IEEE Trans Dielectric Electric Insul*. 2008;15:1031–1037.
8. Inami K, Maeda Y, Habuchi Y, Yoshimura M, Hamano S, Hama H. Problems of the application of N2/SF6 mixtures to gas-insulated bus. *Electr Eng Jpn*. 2001;137:25–31.
9. Yamamoto O, Takuma T, Kinouchi M. Recovery of SF6 from N2/SF6 gas mixtures by using a polymer membrane. *IEEE Electr Insul Mag*. 2002;18:32–37.
10. Toyoda M, Murase H, Imai T, Naotsuka H, Kobayashi A, Takano K, Ohkuma K. SF6 reclaimer from SF6/N2 mixtures by gas separation with molecular sieving effect. *IEEE Trans Power Deliv*. 2003;18:442–448.
11. Murase H, Imai T, Inohara T, Toyoda M. Use of zeolite filter in portable equipment for recovering SF6 in SF6/N2 mixtures. *IEEE Trans Dielectr Electr Insul*. 2004;11:166–173.
12. Shiojiri K, Yanagisawa Y, Yamasaki A, Kiyono F. Separation of F-gases (HFC-134a and SF6) from gaseous mixtures with nitrogen by surface diffusion through a porous Vycor glass membrane. *J Membr Sci*. 2006;282:442–449.
13. Smit B, Maesen TLM. Molecular simulations of zeolites: adsorption, diffusion, and shape selectivity. *Chem Rev*. (Washington, DC, U.S.) 2008;108:4125–4184.
14. Liu B, Wang W, Zhang X. A hybrid cylindrical model for characterization of MCM-41 by density functional theory. *Phys Chem Chem Phys*. 2004;6:3985–3990.
15. Maddox MW, Sowers SL, Gubbins KE. Molecular simulation of binary mixture adsorption in buckytubes and MCM-41. *Adsorption*. 1996;2:23–32.
16. Yun J-H, Duren T, Keil FJ, Seaton NA. Adsorption of methane, ethane, and their binary mixtures on MCM-41: experimental evaluation of methods for the prediction of adsorption equilibrium. *Langmuir*. 2002; 18:2693–2701.
17. Beck JS, Vartuli JC, Roth WJ, Leonowicz ME, Kresge CT, Schmitt KD, Chu CTW, Olson DH, Sheppard EW. A new family of mesoporous molecular sieves prepared with liquid crystal templates. *J Am Chem Soc*. 1992;114:10834–10843.
18. Kresge CT, Leonowicz ME, Roth WJ, Vartuli JC, Beck JS. Ordered mesoporous molecular sieves synthesized by a liquid-crystal template mechanism. *Nature*. 1992;359:710–712.
19. Bhattacharyya S, Lelong G, Saboungi ML. Recent progress in the synthesis and selected applications of MCM-41: a short review. *J Exp Nanosci*. 2006;1:375–395.
20. Brady R, Woonton B, Gee ML, O'Connor AJ. Hierarchical mesoporous silica materials for separation of functional food ingredients—a review. *Innovat Food Sci Emerg Tech*. 2008;9:243–248.
21. Mohanty S, Davis HT, McCormick AV. Shape selective adsorption in cylindrical pores. *Chem Eng Sci*. 2000;55:3377–3383.
22. Matsuoka K, Yamagishi Y, Yamazaki T, Setoyama N, Tomita A, Kyotani T. Extremely high microporosity and sharp pore size distribution of a large surface area carbon prepared in the nanochannels of zeolite Y. *Carbon*. 2005;43:876–879.
23. Kyotani T, Nagai T, Inoue S, Tomita A. Formation of new type of porous carbon by carbonization in zeolite nanochannels. *Chem Mater*. 1997;9:609–615.
24. Gaslain FOM, Parmentier J, Valtchev VP, Patarin J. *First zeolite carbon replica with a well resolved X-ray diffraction pattern*. Chem Commun. (Cambridge, UK) 2006:991–993.

25. Pellenq R, Roussel T, Puibasset J. Molecular simulations of water in hydrophobic microporous solids. *Adsorption*. 2008;14:733–742.
26. Hou P-X, Orikasa H, Itoi H, Nishihara H, Kyotani T. Densification of ordered microporous carbons and controlling their micropore size by hot-pressing. *Carbon*. 2007;45:2011–2016.
27. Roussel T, Bichara C, Gubbins KE, Pellenq RJ-M. Hydrogen storage enhanced in Li-doped carbon replica of zeolites: a possible route to achieve fuel cell demand. *J Chem Phys*. 2009;130:174717.
28. Olivet A, Vega L.F. Optimized molecular force field for sulfur hexafluoride simulations. *J Chem Phys*. 2007;126:144502–144511.
29. Galassi G, Tildesley DJ. Phase diagrams of diatomic molecules using the Gibbs Ensemble Monte Carlo Method. *Mol Simul*. 1994; 13:11–24.
30. Aziz RA, Slaman MJ, Taylor WL, Hurly JJ. An improved intermolecular potential for sulfur hexafluoride. *J Chem Phys*. 1991;94:1034–1038.
31. Neimark AV, Ravikovitch PI, Grün M, Schüth F, Unger KK. Pore size analysis of MCM-41 type adsorbents by means of nitrogen and argon adsorption. *J Colloid Interface Sci*. 1998;207:159–169.
32. Blas FJ, Vega LF. Thermodynamic behaviour of homonuclear and heteronuclear Lennard-Jones chains with association sites from simulation and theory. *Mol Phys*. 1997;92:135–150.
33. Pàmies JC, Vega LF. Vapor-liquid equilibria and critical behavior of heavy *n*-alkanes using transferable parameters from the Soft-SAFT equation of state. *Ind Eng Chem Res*. 2001;40:2532–2543.
34. Olivet A, Vega LF. Predictions of transport properties in gaseous mixtures of sulfur hexafluoride and nitrogen. *J Phys Chem C*. 2007; 111:16013–16020.
35. Tjatjopoulos GJ, Feke DL, Mann JA. Molecule-micropore interaction potentials. *J Phys Chem*. 1988;92:4006–4007.
36. Ravikovitch PI, Vishnyakov A, Neimark AV. Density functional theories and molecular simulations of adsorption and phase transitions in nanopores. *Phys Rev E*. 2001;64:011602.
37. Cao D, Shen Z, Chen J, Zhang X. Experiment, molecular simulation and density functional theory for investigation of fluid confined in MCM-41. *Microporous Mesoporous Mater*. 2004;67:159–166.
38. Herdes C, Santos MA, Abelló S, Medina F, Vega LF. Search for a reliable methodology for PSD determination based on a combined molecular simulation-regularization-experimental approach: the case of PHTS materials. *Appl Surf Sci*. 2005;252:538–547.
39. Herdes C, Santos MA, Medina F, Vega LF. Pore size distribution analysis of selected hexagonal mesoporous silicas by grand canonical Monte Carlo simulations. *Langmuir*. 2005;21:8733–8742.
40. Neimark AV, Ravikovitch PI, Vishnyakov A. Adsorption hysteresis in nanopores. *Phys Rev E*. 2000;62:R1493.
41. Ravikovitch PI, Haller GL, Neimark AV. Density functional theory model for calculating pore size distributions: pore structure of nanoporous catalysts. *Adv Colloid Interface Sci*. 1998;76–77:203–226.
42. Roussel T, Didion A, Pellenq RJ-M, Gadiou R, Bichara C, Vix-Guterl C. Experimental and atomistic simulation study of the structural and adsorption properties of faujasite zeolite–templated nanostructured carbon materials. *J Phys Chem C*. 2007;111:15863–15876.
43. Roussel T, Bichara C, Gubbins KE, Pellenq RJ-M. Hydrogen storage enhanced in Li-doped carbon replica of zeolites: a possible route to achieve fuel cell demand. *J Chem Phys*. 2009;130:174717.
44. Kuznetsova A, Yates JT, Simonyan VV, Johnson JK, Huffman CB, Smalley RE. Optimization of Xe adsorption kinetics in single walled carbon nanotubes. *J Chem. Phys*. 2001;115:6691–6698.
45. Frenkel D, Smit B. *Understanding Molecular Simulation*, 2nd ed. San Diego, CA: Academic Press, 2001.
46. Duque D, Vega LF. Some issues on the calculation of interfacial properties by molecular simulation. *J Chem Phys*. 2004;121:8611–8617.
47. Gallo M, Glossman-Mitnik D. Fuel gas storage and separations by metal-organic frameworks: simulated adsorption isotherms for H2 and CH4 and their equimolar mixture. *J Phys Chem C*. 2009;113: 6634–6642.
48. Talbot J. Analysis of adsorption selectivity in a one-dimensional model system. *AIChE J*. 1997;43:2471–2478.
49. Jiang J, Sandler SI. Monte Carlo simulation of O2 and N2 mixture adsorption in nanoporous carbon (C168 Schwarzite). *Langmuir*. 2003;19:5936–5941.
50. Somers SA, McCormick AV, Davis HT. Superselectivity and solvation forces of a two component fluid adsorbed in slit micropores. *J Chem Phys*. 1993;99:9890–9898.
51. Yang Q, Xue C, Zhong C, Chen J-F. Molecular simulation of separation of CO2 from flue gases in CU-BTC metal-organic framework. *AIChE J*. 2007;53:2832–2840.
52. Heyden A, Düren TJ, Keil F. Study of molecular shape and nonideality effects on mixture adsorption isotherms of small molecules in carbon nanotubes: a grand canonical Monte Carlo simulation study. *Chem Eng Sci*. 2002;57:2439–2448.
53. Babarao R, Hu Z, Jiang J, Chempath S, Sandler SI. Storage and separation of CO2 and CH4 in silicalite, C168 Schwarzite, and IRMOF-1: a comparative study from Monte Carlo simulation. *Langmuir*. 2006;23:659–666.
54. Bhatia SK, Tran K, Nguyen TX, Nicholson D. High-pressure adsorption capacity and structure of CO2 in carbon slit pores: theory and simulation. *Langmuir*. 2004;20:9612–9620.
55. Do DD, Do HD. Adsorption of quadrupolar, diatomic nitrogen onto graphitized thermal carbon black and in slit-shaped carbon pores. Effects of surface mediation. *Adsorp Sci Technol*. 2005;23:267–288.
56. Lobo RF. Chemistry: the promise of emptiness. *Nature*. 2006;443: 757–758.
57. Gallo M, Nenoff TM, Mitchell MC. Selectivities for binary mixtures of hydrogen/methane and hydrogen/carbon dioxide in silicalite and ETS-10 by Grand Canonical Monte Carlo techniques. *Fluid Phase Equilib*. 2006;247:135–142.
58. Liu B, Yang Q, Xue C, Zhong C, Chen B, Smit B. Enhanced adsorption selectivity of hydrogen/methane mixtures in metalic-organic frameworks with interpenetration: a molecular simulation study. *J Phys Chem C*. 2008;112:9854–9860.

Manuscript received Sept. 25, 2009, revision received Mar. 21, 2010, and final revision received May 18, 2010.